

Theory of a high frequency magnetic tunable filter and phase shifter

R. J. Astalos and R. E. Camley

Department of Physics, University of Colorado at Colorado Springs, Colorado Springs, Colorado 80933-7150

(Received 3 September 1997; accepted for publication 24 November 1997)

Microwave propagation in a layered dielectric/ferromagnet were explored in the past. Previous studies, however, made use of an approximation to the full permeability tensor in the ferromagnet. This approximation fails in a frequency range where the structure can act as a band pass filter. Here we seek to verify the behavior in the predicted band pass region using the full permeability tensor. We also explore the use of the layered structure in two devices: a tunable band pass filter and an adjustable phase shifter. © 1998 American Institute of Physics. [S0021-8979(98)05405-X]

I. INTRODUCTION

Recently there has been increasing interest in signal processing in higher frequency ranges, 20 GHz and above. While magnetic insulators such as yttrium iron garnet (YIG) have long been used for lower frequency applications, such materials require large external magnetic fields to operate at higher frequencies. To overcome this problem, a number of publications have suggested the use of thin metallic films of Fe,¹⁻⁴ or other metallic magnets.⁵

The primary reason that Fe, e.g., might be preferred over YIG is that it has a much higher saturation magnetization, M_s . To a large extent M_s determines the typical operating frequency since the resonance frequency of a simple ferromagnetic thin film is given by $\omega = \gamma \sqrt{H_0(H_0 + 4\pi M_s)}$. Clearly Fe, with a M_s of about 1.7 kG, will have a much higher operating frequency than YIG with a M_s of 0.16 kG.

Unfortunately, the fact that Fe is a metal causes difficulties, since induced currents in the Fe can cause energy losses which result in significant damping of electromagnetic waves. Furthermore, these same currents tend to screen out electromagnetic waves giving a skin depth on the order of 1 μm . Thus, use of Fe in signal processing has been limited to films of 1 μm or thinner.

Despite these difficulties, there have been a number of initial studies, both experimental and theoretical, using thin Fe films as the active element in a signal processing application. For example, Schloemann^{1,2} showed that a notch filter could be fabricated on a GaAs/Fe based structure, which could operate in the 15–20 GHz range with an applied field on the order of 1–2 kG. Some recent theoretical work indicates that a tunable band pass filter, operating around 60 GHz, can be constructed using essentially the same design.³

The theoretical calculations in Refs. 1–4 approximate the magnetic permeability tensor in Fe with a diagonal tensor. This approximation is valid near resonance, where the skin depth is less than a micron. However, in the band pass region the skin depth becomes much larger and the approximation becomes suspect.

Our first goal in this article, therefore, is to complete a calculation for the band pass filter without recourse to the approximation used previously. Thus we use the full permeability tensor to describe the magnetic material. This causes

a significant increase in the complexity of the calculation, but is necessary to validate the existence of the band pass region.

We have two additional goals. First, we want to explore how the band pass filter characteristics depend on material parameters, such as the conductivity of the Fe and the thickness of the different films in the filter. Second, we explore whether the filter structure could also be used as an adjustable phase shifter.

Our results are very encouraging. Using the full permeability matrix has made it possible to show that the band pass region does, indeed, exist, and its structure is very similar to that anticipated in earlier studies. It has also allowed us to demonstrate the extent to which the shape of the region responds to changes in the material. The width, minimum attenuation, and center frequency of the region can all be modified. Finally, parameter values which would allow the filter to act as a phase shifting device have been found, demonstrating that other applications of the device are possible.

The structure of the article is as follows: In Sec. II the theoretical calculations are briefly outlined. Section III presents our numerical results and their possible application to devices. Section IV contains concluding remarks.

II. THEORY

The geometry of the filter structure is illustrated in Fig. 1. A dielectric layer of thickness D sits on top of a layer of silver. It is covered by an iron layer of thickness d , which is then covered by another silver layer. For convenience we define our coordinates such that all interfaces are parallel to the xz -plane. The Fe/dielectric interface is chosen to be at $y=0$, so the bottom of the dielectric layer is at $y=-D$, and the top of the Fe layer is at $y=d$. Edge effects will be ignored in the x direction; that is, we treat the structure as if it extends from $x=-\infty$ to $x=+\infty$.

The microwaves propagate along the z -axis with wave vector k_z . There is a k_y component, as well. However, by symmetry, $k_x=0$. There is a constant external magnetic field \mathbf{H}_0 applied parallel to the z -axis.

Our goal is to describe the propagation of electromagnetic waves in our device. That is, we want to determine the propagation vector \mathbf{k} for a given frequency ω . As usual, the

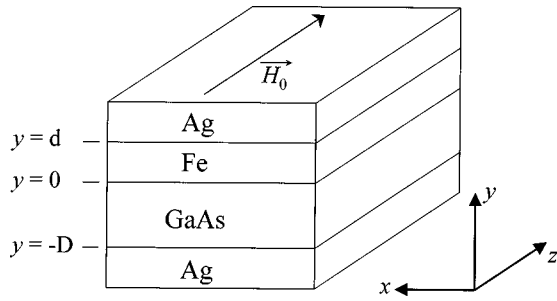


FIG. 1. Geometry of the filter structure. A dielectric layer and magnetic layer are surrounded by layers of Ag. An external field is applied along the +z direction, parallel to the propagation direction.

real part of k_z will determine the phase of the wave, while the imaginary part governs attenuation. Thus examination of \mathbf{k} as a function of ω gives the information necessary to predict the behavior of both the band pass filter and the phase shifter.

We will start with Maxwell's equations applied to the ferromagnet, developing a relationship involving the components of \mathbf{H} . This will allow us to analytically determine the k_y values that go with a particular value of k_z and ω . The number of k_y values gives the number of independent electromagnetic modes allowed in the ferromagnet. For each mode, we obtain the components of \mathbf{E} and \mathbf{H} in terms of a single variable through Maxwell's equations. At the end, we form a superposition of these modes to represent the total field in the ferromagnet.

This analysis will then be repeated in the dielectric, stressing the differences in the results. Once all the components in both layers have been represented in terms of the independent variables, we will discuss the boundary conditions used. These will be used to write a matrix equation $\mathbf{R}\mathbf{v}=\mathbf{0}$, where \mathbf{R} is our "boundary condition matrix," and \mathbf{v} is the vector of independent variables. This has a nontrivial solution *only* if the determinant of \mathbf{R} is zero. Since the only unknown in \mathbf{R} is the value of k_z , k_z can be found by conventional root finding techniques. This process is then repeated for each value of ω in the frequency range of interest.

The permeability tensor in Fe used for this analysis is of the form

$$\boldsymbol{\mu} = \begin{bmatrix} \mu_1 & i\mu_T & 0 \\ -i\mu_T & \mu_1 & 0 \\ 0 & 0 & 1 \end{bmatrix} \quad (1)$$

with

$$\mu_1 = 1 + \frac{4\pi\gamma M_S(\gamma H_0 - i\Gamma\omega)}{(\gamma H_0 - i\Gamma\omega)^2 - \omega^2}, \quad (2)$$

$$\mu_T = \frac{4\pi\gamma M_S\omega}{(\gamma H_0 - i\Gamma\omega)^2 - \omega^2}, \quad (3)$$

where γ is the gyromagnetic ratio.

The dimensionless parameter Γ stems from dissipation in the spin system. The ferromagnetic resonance line width, ΔH , depends upon it in the following way:^{6,7}

$$\Delta H = 1.16 \left(\frac{\omega}{\gamma} \right) \Gamma, \quad (4)$$

where ΔH is in kG and γ is 2.87 GHz/kG.

The permittivity tensor is of the form

$$\boldsymbol{\epsilon} = \begin{bmatrix} \epsilon & 0 & 0 \\ 0 & \epsilon & 0 \\ 0 & 0 & \epsilon \end{bmatrix} \quad (5)$$

for both the Fe and dielectric layers. In Fe, $\epsilon_m(\omega) = 1 + i\sigma/\epsilon_0\omega$, where σ will be varied from 1×10^5 to $1 \times 10^8 \Omega^{-1} \text{m}^{-1}$. For the dielectric, we chose $\epsilon_d \approx 11.7$, which is close to that of GaAs.

We begin with an analysis of the waves in the iron layer. Using the two Maxwell curl equations and the relations

$$\mathbf{D} = \boldsymbol{\epsilon}\mathbf{E}, \quad (6)$$

$$\mathbf{B} = \boldsymbol{\mu}\mathbf{H}, \quad (7)$$

we obtain

$$\nabla \times (\boldsymbol{\epsilon}^{-1} \nabla \times \mathbf{H}) = -\frac{1}{c^2} \frac{\partial^2}{\partial t^2} (\boldsymbol{\mu}\mathbf{H}). \quad (8)$$

In order to evaluate the derivatives we assume a wave of the form $Ae^{i(\mathbf{k}\cdot\mathbf{x} - \omega t)}$. The position derivatives each introduce a factor of ik_j , where the j represents x , y , or z , appropriately. The time derivatives each introduce a factor of $-i\omega$. Thus, Eq. (8) becomes

$$\begin{aligned} & \hat{i} \left[\frac{1}{\epsilon} (-k_y k_x H_y - k_z k_x H_z + k_y^2 H_x + k_z^2 H_x) \right] \\ & + \hat{j} \left[\frac{1}{\epsilon} (-k_z k_y H_z - k_x k_y H_x + k_z^2 H_y + k_x^2 H_y) \right] \\ & + \hat{i} \left[\frac{1}{\epsilon} (-k_x k_z H_x - k_y k_z H_y + k_x^2 H_z + k_y^2 H_z) \right] \\ & = \hat{i} \left[\frac{\omega^2}{c^2} H_x \mu_1 + \frac{\omega^2}{c^2} H_y \mu_T \right] \\ & + \hat{j} \left[-\frac{\omega^2}{c^2} H_x \mu_T + \frac{\omega^2}{c^2} H_y \mu_1 \right] + \hat{k} \left[\frac{\omega^2}{c^2} H_z \right]. \end{aligned} \quad (9)$$

Noting that $k_x=0$, several terms vanish. This can be written in the matrix form $\mathbf{Q}\mathbf{H}=\mathbf{0}$:

$$\begin{bmatrix} \frac{k_y^2}{\epsilon} + \frac{k_z^2}{\epsilon} - \frac{\mu_1 \omega^2}{c^2} & -\frac{i\mu_T \omega^2}{c^2} & 0 \\ \frac{i\mu_T \omega^2}{c^2} & \frac{k_z^2}{\epsilon} - \frac{\mu_1 \omega^2}{c^2} & -\frac{k_y k_z}{\epsilon} \\ 0 & -\frac{k_y k_z}{\epsilon} & \frac{k_y^2}{\epsilon} - \frac{\omega^2}{c^2} \end{bmatrix} \begin{bmatrix} H_x \\ H_y \\ H_z \end{bmatrix} = \begin{bmatrix} 0 \\ 0 \\ 0 \end{bmatrix}, \quad (10)$$

which has a nontrivial solution only if the determinant of \mathbf{Q} is zero. $|\mathbf{Q}|=0$, then, is an expression which can be used to analytically determine the value of k_y for a given k_z :

$$k_y^4 \left[-\frac{\mu_1 \omega^2}{\epsilon^2 c^2} \right] + k_y^2 \left[\frac{\omega^4}{\epsilon c^4} (\mu_1 + \mu_1^2 - \mu_T^2) - \frac{k_z^2 \omega^2}{\epsilon^2 c^2} (1 + \mu_1) \right] + \left[\frac{2\mu_1 k_z^2 \omega^4}{\epsilon c^4} - \frac{k_z^4 \omega^2}{\epsilon^2 c^2} + \frac{\omega^6}{c^6} (\mu_T^2 - \mu_1^2) \right] = 0. \quad (11)$$

The relationship is a simple quadratic in k_y^2 , so analytical solutions are readily found. For a given k_z , there are four k_y roots, and therefore, four independent variables. We write the total H_x as a linear superposition of the four waves with different k_y 's:

$$H_x = \sum_{j=1}^4 A(j) e^{ik_y(j)y} e^{ik_z z}, \quad (12)$$

where the $A(j)$ are the independent variables.

We also use \mathbf{Q} to write H_y and H_z in terms H_x , and then in terms of the $A(j)$:

$$H_y = \sum_{j=1}^4 \alpha(j) A(j) e^{ik_y(j)y} e^{ik_z z}, \quad (13)$$

$$H_z = \sum_{j=1}^4 \beta(j) A(j) e^{ik_y(j)y} e^{ik_z z}, \quad (14)$$

where the α 's and β 's are determined from the \mathbf{Q} matrix through Eq. (10).

We now express the components of \mathbf{E} in terms of H_x , H_y , and H_z , and thus, in terms of our independent variables. Maxwell's equation for the curl of \mathbf{H} can be written

$$\epsilon^{-1} \nabla \times \mathbf{H} = \frac{1}{c} \frac{\partial \mathbf{E}}{\partial t}. \quad (15)$$

Working out the derivatives,

$$\frac{i}{\epsilon} (k_y H_z - k_z H_y) = -\frac{i\omega}{c} E_x, \quad (16)$$

$$\frac{i}{\epsilon} (k_z H_x - k_x H_z) = -\frac{i\omega}{c} E_y, \quad (17)$$

$$\frac{i}{\epsilon} (k_x H_y - k_y H_x) = -\frac{i\omega}{c} E_z. \quad (18)$$

We now solve these for E_x , E_y , and E_z and write them in terms of the $A(j)$ (remembering $k_x = 0$).

$$E_x = \frac{c}{\epsilon\omega} \sum_{j=1}^4 \{ [k_z \alpha(j) - k_y(j) \beta(j)] A(j) e^{ik_y(j)y} e^{ik_z z} \}, \quad (19)$$

$$E_y = -\frac{c}{\epsilon\omega} \sum_{j=1}^4 [k_z A(j) e^{ik_y(j)y} e^{ik_z z}], \quad (20)$$

$$E_z = \frac{c}{\epsilon\omega} \sum_{j=1}^4 [k_y(j) A(j) e^{ik_y(j)y} e^{ik_z z}]. \quad (21)$$

At this point all six components, H_x , H_y , H_z , E_x , E_y , and E_z , in the Fe layer are written in terms of the four independent variables $A(j)$. In order to make use of the boundary conditions, a corresponding analysis must be done

in the dielectric, deriving expressions for the k_y 's and writing the \mathbf{E} and \mathbf{H} components in terms of independent variables.

In the dielectric, the permeability tensor is simply $\boldsymbol{\mu} = \mathbf{I}$, which produces a somewhat simplified \mathbf{Q} matrix:

$$\begin{bmatrix} \frac{k_y^2}{\epsilon} + \frac{k_z^2}{\epsilon} - \frac{\omega^2}{c^2} & 0 & 0 \\ 0 & \frac{k_z^2}{\epsilon} - \frac{\omega^2}{c^2} & -\frac{k_y k_z}{\epsilon} \\ 0 & -\frac{k_y k_z}{\epsilon} & \frac{k_y^2}{\epsilon} - \frac{\omega^2}{c^2} \end{bmatrix} \begin{bmatrix} H_x \\ H_y \\ H_z \end{bmatrix} = \begin{bmatrix} 0 \\ 0 \\ 0 \end{bmatrix}. \quad (22)$$

Because \mathbf{Q} is block diagonal, we get two separate conditions which determine k_y values for a given k_z . The first condition comes from the (1,1) element of \mathbf{Q} :

$$\frac{k_y^2}{\epsilon} + \frac{k_z^2}{\epsilon} - \frac{\omega^2}{c^2} = 0. \quad (23)$$

This represents the k_y 's of the wave's transverse magnetic mode. Since this expression is quadratic, we will get two k_y values, which we will label with a superscript 1 to avoid confusion with the previous four k_y 's. The second condition is that the determinant of the lower right 2×2 submatrix must be zero. This represents the k_y 's of the wave's transverse electric mode, and is mathematically equivalent to the first condition. Though the k_y values themselves are the same, they do represent two additional independent variables because they exist simultaneously in a separate mode. Therefore, these two k_y values will be superscript 2.

The block diagonal character of \mathbf{Q} also means that we cannot express H_y and H_z in terms of H_x . Instead, we write H_x in terms of the first two independent variables:

$$H_x = \sum_{j=1}^2 B(j) e^{ik_y^{(1)}(j)y} e^{ik_z z}. \quad (24)$$

We then write H_y in terms of the second pair of independent variables:

$$H_y = \sum_{j=1}^2 C(j) e^{ik_y^{(2)}(j)y} e^{ik_z z}, \quad (25)$$

and H_z in terms of H_y :

$$H_z = \sum_{j=1}^2 \delta(j) C(j) e^{ik_y^{(2)}(j)y} e^{ik_z z}, \quad (26)$$

where the δ 's are determined from \mathbf{Q} .

We express the components of \mathbf{E} in terms of the independent variables in the dielectric in the same manner as in the ferromagnet. The result is

$$E_x = \frac{c}{\epsilon\omega} \sum_{j=1}^2 \{ [k_z - k_y^{(2)}(j) \delta(j)] C(j) e^{ik_y^{(2)}(j)y} e^{ik_z z} \}, \quad (27)$$

$$E_y = -\frac{c}{\epsilon\omega} \sum_{j=1}^2 [k_z B(j) e^{ik_y^{(1)}(j)y} e^{ik_z z}], \quad (28)$$

$$E_z = \frac{c}{\epsilon\omega} \sum_{j=1}^2 [k_y^{(1)}(j) B(j) e^{ik_y^{(1)}(j)y} e^{ik_z z}]. \quad (29)$$

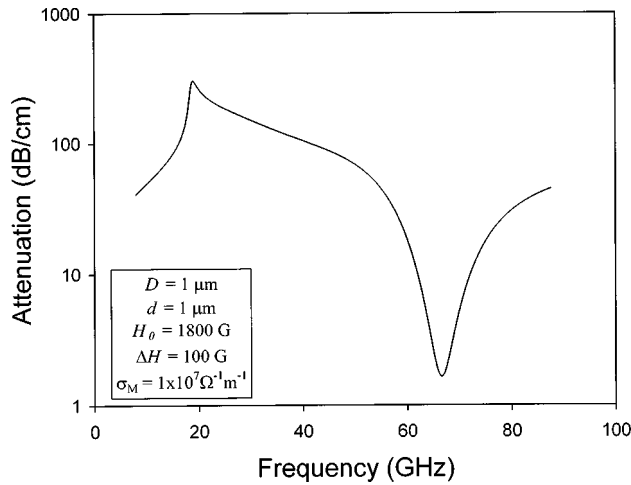


FIG. 2. Attenuation vs frequency for typical material parameters. The band pass region is clearly visible above 60 GHz.

We now have all **E** and **H** components written in terms of eight independent variables: the four *A*'s, two *B*'s, and two *C*'s. Because we have eight independent variables, we will need eight boundary conditions. We use the standard condition at an interface that the tangential components of **E** and **H** must be continuous, along with the approximation that the waves do not enter the silver layer. At $y=d$, there are two conditions: $E_x=0$ and $E_z=0$. At $y=0$, there are four: $E_x, E_z, H_x,$ and H_z in the ferromagnet are equal to $E_x, E_z, H_x,$ and H_z in the dielectric. Finally, at $y=-D$, there are two: $E_x=0$ and $E_z=0$. Writing these eight equations in terms of the eight independent variables as given above, and expressing them in matrix form yields $\mathbf{R}\mathbf{v}=\mathbf{0}$, which, again, has a nontrivial solution only if $|\mathbf{R}|=0$.

The problem is now reduced to finding the value of k_z which, for a given ω , satisfies $|\mathbf{R}|=0$. This is a root-finding problem, requiring an initial guess at the value of the root. Our approach was to use the analytical solution to a geometry with no iron layer as an initial guess. We were able to generate results over the entire frequency range of interest, for higher modes as well as the lowest. We then turned to a model presented by Schloemann, and found it to be highly accurate, although only suitable for producing the lowest mode.

III. NUMERICAL RESULTS AND APPLICATIONS

As noted in the introduction, earlier treatments of the problem depended on an approximation, the validity of which is not obvious in the band pass region. Our first objective, therefore, was to verify the behavior of the device in the band pass region. We found it useful to display our results using semi-log graphs such as Fig. 2, which presents a typical attenuation curve. The band pass region is clearly demonstrated.

The ability to alter the shape of the band pass region is crucial in designing a filter for a specific application. For that reason, we studied the effect of dielectric thickness, ferromagnet thickness, external field, ferromagnet conductivity, and FMR line width on the depth and width of the attenua-

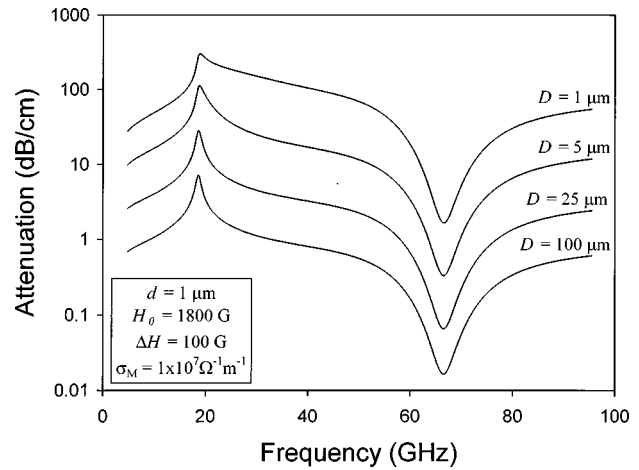


FIG. 3. Effect of dielectric thickness on attenuation. A thicker dielectric layer provides significantly less attenuation.

tion curve. We found that the shape of the band pass region can be adjusted to a great extent by varying the physical parameters of the system.

The thickness of the dielectric layer has a significant impact on attenuation. As shown in Fig. 3, a dielectric thickness of 100 μm provides one hundred times less attenuation in the band pass region than a thickness of 1 μm , holding all other parameters constant. A band pass filter would have a lower minimum attenuation with a thicker dielectric layer. The width of the region is not greatly affected.

The skin depth of iron is on the order of 1 μm ; therefore, increasing the ferromagnet layer thickness beyond 1 μm has little effect on attenuation. However, *decreasing* the thickness of that layer not only reduces attenuation, but also greatly broadens the width of the band pass region and shifts the minimum attenuation to a slightly higher frequency, as seen in Fig. 4.

The applied magnetic field has only a very slight effect on minimum attenuation; it's main influence is to shift the center of the band pass region in frequency, as seen in Fig. 5. Fields varying from 10 to 1800 G result in a band center

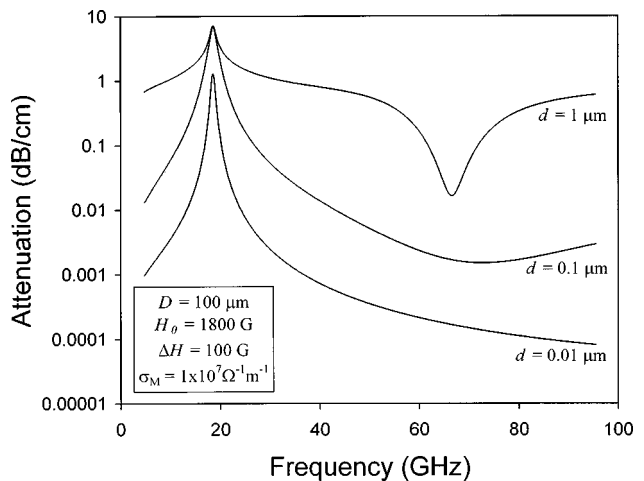


FIG. 4. Effect of ferromagnet thickness on attenuation. A decrease in thickness decreases attenuation, but also widens the region significantly.

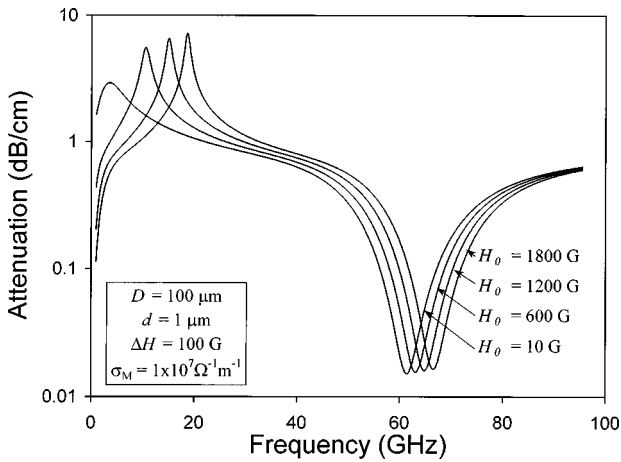


FIG. 5. Effect on attenuation of varying the external field. The shift in frequency of the band pass region makes a tunable filter possible. Note that the shape of the region is not appreciably affected.

from 61 to 67 GHz. This shift provides the possibility of making the band pass filter tunable. The frequency shift from the zero field value is given simply by γH_0 .

The change in attenuation with ferromagnet conductivity is quite interesting. Figure 6 shows that in the band pass region, increasing the conductivity reduces the width of the band. Therefore, a band pass filter can be designed with a much higher Q using a higher conductivity in the ferromagnet.

Finally, it is interesting to note that, in contrast to the usual situation, FMR line width has very little effect on the width of the band pass region. Varying the line width primarily alters the minimum attenuation, as seen in Fig. 7. Outside of the band pass region, the effect is negligible.

Another possible device application for this structure is an adjustable phase shifter. With zero external field, the signal's phase upon exiting the device is some value, ϕ . Application of a nonzero external field causes the phase upon exit to be $\phi + \delta$. If we can choose the material parameters such that $\delta \cong \pm \pi$, then the device could act as an adjustable phase shifter. In the graphs that follow, the quantity labeled "phase difference" is δ for an external field of 1800 G.

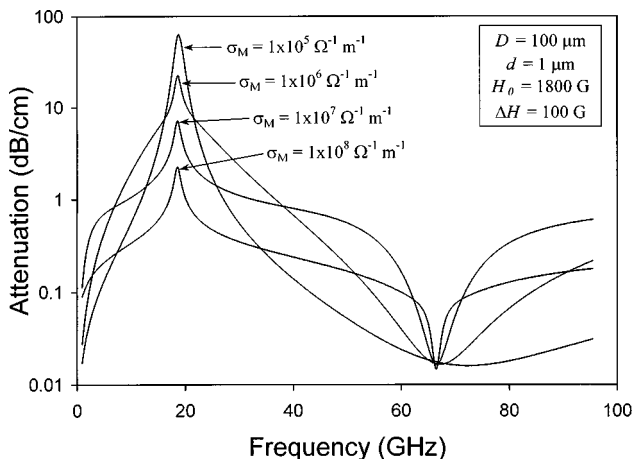


FIG. 6. Effect of ferromagnet conductivity on attenuation. High conductivity causes a sharp decrease in the width of the band pass region.

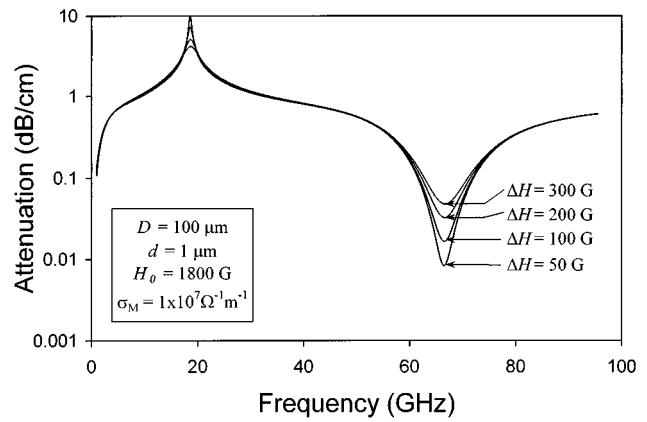


FIG. 7. Effect of ferromagnetic resonance line width on attenuation. It is interesting that the width of the band pass region is not affected. Only the minimum attenuation changes with line width.

One further requirement is necessary if the device is to be useful: the attenuation through the length of the device must be sufficiently low, say 1–2 dB. Since the attenuation is lowest in the band pass region, it is reasonable to focus on that frequency range in our search.

As noted above, a thicker dielectric layer provides a lower attenuation. However, for a phase shifter, the effect on phase change must also be considered. While a thinner layer produces a higher attenuation, Fig. 8 shows that it also produces a greater phase change—a π phase-shifter could be made of a shorter length device if a thinner dielectric layer is used. Reducing the thickness of the ferromagnet layer also reduces attenuation. However, it is seen in Fig. 9 that it produces *less* of a phase change, requiring a greater length device to achieve the same phase shift.

We have seen that the external magnetic field can alter the center frequency of the band pass region. Therefore, for our adjustable phase shifter to be useful, the band pass region

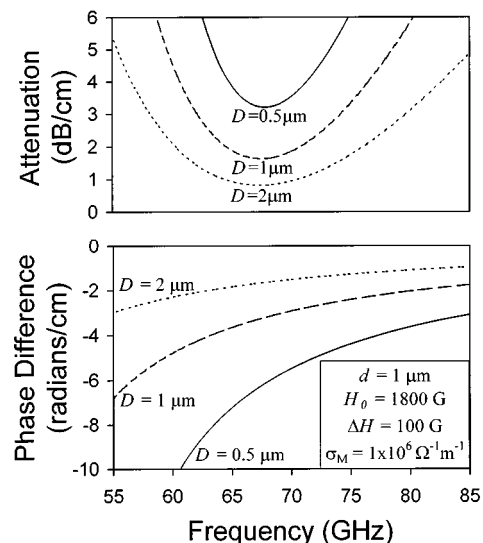


FIG. 8. Effect of dielectric thickness on attenuation and phase change. Note that the increase in attenuation with a thinner layer is offset to a great extent by the increase in phase difference.

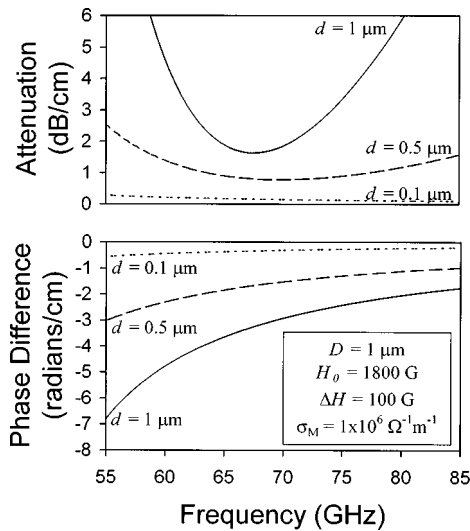


FIG. 9. Effect of ferromagnet thickness on attenuation and phase change. A thicker layer increases attenuation, but also increases the phase difference.

will have to be fairly wide so that the attenuation is low over all values of H_0 . Since decreasing ferromagnet conductivity increases the width of the band pass region, a low conductivity ferromagnet is desirable. That lower conductivity also improves the phase change as seen in Fig. 10. A phase shifter will therefore benefit from a lower conductivity in multiple ways.

It was shown above that a lower FMR line width reduces the minimum attenuation in the band pass region. This is obviously useful for an adjustable phase shifter. Our calculations show that the phase shift is not appreciably affected by the line width.

For an adjustable phase shifter, the attenuation should remain below some reasonable value over the entire range of external fields. In Fig. 11 we study attenuation and phase

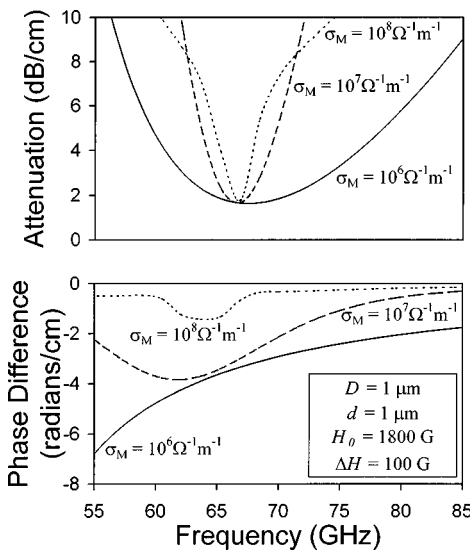


FIG. 10. Effect of ferromagnet conductivity on attenuation and phase change. The lower conductivity broadens the band pass region and increases the phase difference, both important for a useful phase shifter.

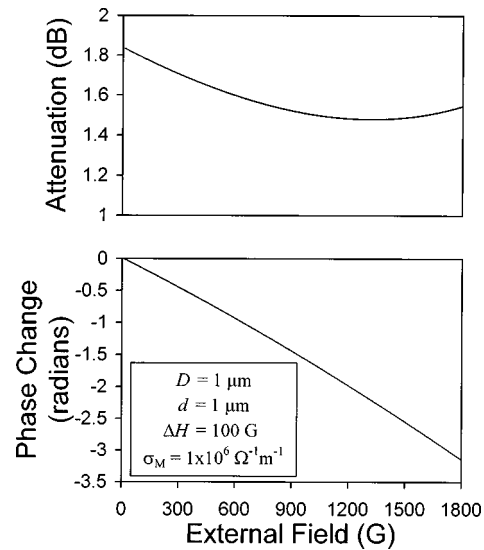


FIG. 11. Attenuation and phase difference over a range of external fields. A reasonable attenuation and a maximum phase difference of π make an adjustable phase shifter feasible.

shift as a function of applied field. The frequency is set to 66.5 GHz and we take the length of the device to be 0.92 cm. We see that the phase can be changed continuously from 0 to π , and the attenuation kept below 1.7 dB over most of the range.

IV. CONCLUSIONS

We have been able to verify the behavior of our device in the band pass region, without resorting to the approximation which, in past analyses, was suspect precisely in the region of interest. The approximation due to Schloemann proved to be very accurate at all frequencies studied. It has also been shown that the shape of the band pass region can be modified by adjustment of the physical parameters: the width of the region, the minimum attenuation, even the center frequency, can all be controlled. These results suggest that a tunable band pass filter is viable at the higher frequencies desired in signal processing. Other devices, such as the adjustable phase shifter we demonstrated, may also be possible using iron/insulator layers.

ACKNOWLEDGMENTS

The work of R.J.A. was supported by U.S. ARO Grant No. DAA H04-94-G-0253. One of the authors (R.E.C.) was supported by the ARO under Grant No. CS0013132.

- ¹E. Schloemann, R. Tutison, J. Weissman, H. J. Van Hook, and T. Vati-mos, *J. Appl. Phys.* **63**, 3140 (1988).
- ²V. S. Liau, T. Wong, W. Stacey, S. Ali, and E. Schloemann, *IEEE MTT-S Dig.* 957 (1991)
- ³R. E. Camley and D. L. Mills, *J. Appl. Phys.* **82**, 3058 (1997).
- ⁴O. Acher, P. M. Jacquart, J. M. Fontaine, P. Baclet, and G. Perrin, *IEEE Trans. Magn.* **30**, 4533 (1994).
- ⁵A. J. Sievers, *J. Appl. Phys.* **41**, 980 (1970).
- ⁶In the conventional form of the Landau–Lifshitz equations, one encounters the Gilbert damping constant G (Ref. 7). We have $\Gamma = G/\gamma M_s \equiv G/\Omega_M$. For Fe at room temperature, $G = 0.8 \times 10^8 \text{ s}^{-1}$.
- ⁷B. Heinrich and J. F. Cochran, *Adv. Phys.* **42**, 523 (1993).